



Singularities of Taylor's power law in the analysis of aggregation measures

Samuele De Bartolo

Department of Engineering for Innovation, EUMER, University of Salento, via per Monteroni, S.P.6, Lecce, 73100, Italy

ARTICLE INFO

Keywords:

Taylor's power law
Poissonian processes
Aggregate measures

ABSTRACT

Taylor's law is a well-known power law (TPL) for analysing the scaling behaviour of many fluctuating physical phenomena in nature. The scaling exponent b of this law forms the basis of the aggregation process to which a precise probability density function corresponds. In some phenomena, TPL behaviour with periodic components of the aggregates has been observed for small partitions, especially for physical processes characterised by values of $b = 1$ where fluctuation-related aggregation processes are supported by Poissonian distributions. We intend to show that for values of b very close to unity it is possible to find a trend, in the double logarithmic scale, of the TPL that there are 'periodic patterns' (components) between variance and mean. This behaviour is found in other binomial-type distributions, of which the Poissonian is a particular case, with mappings characterised by a variance close to 1.

1. Introduction

L.R. Taylor's 1961 pioneering work [1] based on a power law (TPL) of the type $\sigma^2 = a\mu^b$ made it possible to reveal, in terms of aggregates, a very large number of physical and biological quantities and their scaling fluctuations [2]. Variance, σ^2 , and mean, μ , of these fluctuations are correlated through a constant, a , and a scaling exponent or 'index of aggregation', b . The latter, once estimated, allows us to define the probability density functions that supports measurement of fluctuations in a suitable manner [3]. It has been widely shown [3–12] that for $b = 1$ the scaling processes of the fluctuations are governed by Poissonian probability density functions. In the cases $b = 2$ and $b = 0$ the processes are supported by Gamma and Gaussian distributions. The range of values between 1 and 2 is especially interesting, as the processes are supported by Tweedie distributions [3]. These constitute a subset of a family of probability distributions called Exponential Dispersion Models (EDMs) [13]. Such probability distributions do not exist in the range of values between 1 and 0 [3]. In both discriminating fields, it is of fundamental importance to understand the scaling behaviour of the fluctuations, i.e. whether they are simple-scaling ($b \rightarrow \text{const}$) or multiscaling ($b \neq \text{const}$) in nature and their spatial or temporal aggregates [8,9,11,14]. Alongside these well-known properties of TPL, further properties have emerged since the work of Taylor and Woiwod [15] on the life dynamics of certain animal species, Hughes and Madden [16] in the context of research on aggregation and incidence of disease in virus-infected crops of tobacco, De Bartolo et al. [14] and Rizzello et al. [17] within the river dynamics of braided systems, which have revealed a singular behaviour of the same law with 'periodic components'. In the current state of knowledge, these periodic patterns have not yet been sufficiently analysed. In the context of this work, we shall refer to them as singularities. Although these periodic patterns emerge in different environments, and are presumably dependent on the individual physical phenomena analysed, they have not been attributed to intrinsic properties of the probability density functions (distributions) that support TPLs. The aim of this work is to demonstrate that the emergence of periodic components within certain

E-mail address: samuele.debartolo@unisalento.it.

<https://doi.org/10.1016/j.physa.2024.130151>

Received 15 July 2024; Received in revised form 3 October 2024

Available online 10 October 2024

0378-4371/© 2024 The Author. Published by Elsevier B.V. This is an open access article under the CC BY-NC-ND license (<http://creativecommons.org/licenses/by-nc-nd/4.0/>).

TPLs depends on probability density functions that can be attributed to the binomial type, including the Poissonian one, the latter being a limiting case of the previous and similar asymptotic ones. This dependency becomes relevant as long as the difference between the variance, σ^2 , and the mean, μ , of the partitioned aggregates within the TPL remains smaller than a certain threshold value. The direct observation of numerical simulations, carried out on a synthetic set of data generated through the above-mentioned distributions, made it possible to identify the region of the TPL where the periodic components manifest themselves. This region is a range for which the values of the variances, σ^2 , lie between 0 and an upper limit very close to the unity. This numerical analysis was supplemented by an experimental analysis on a further real case which confirmed the same behaviour. This investigation was carried out as described in De Bartolo et al. [14] and Rizzello et al. [17] on a braided channel system of the Allaro River.

2. Singularities in the Taylor's power law

2.1. TPL cases with Poisson and Bernoulli distributions

As anticipated in Section 1, some TPLs may have special configurations with some singularities. Historically, there are traces of periodic components in TPL in the works of Taylor and Woiwod [15], and Hughes and Madden [16]. The latter characterised by Bernoulli distributions. Specifically, for a random variable, X , with a non-zero mean μ , for $b = 1$, aggregate measures will have a support characterised by a probability density function, $P(X, \lambda)$, consisting of a Poissonian distribution, i.e.:

$$P(X, \lambda) = \frac{\lambda^X}{X!} \exp(-\lambda) \quad (1)$$

that is a one-parameter distribution, where the unique scale parameter λ represents both the mean and the variance ($\sigma^2 = \mu$). The more recent literature, essentially based on the work of Eliazar [18,19], provides interesting power-law approaches to the analysis of harmonic statistics obtainable from Poissonian distributions, but has not yet offered any connection with harmonic patterns obtainable from TPL with aggregation processes of physical phenomena characterised by fluctuation measures. It is important to note that in the presence of fluctuating physical phenomena characterised by small groups of spatial or temporal measurements, with Poissonian distributions ($b = 1$), the behaviour of the TPL, i.e. σ^2 versus μ , can assume a periodic mapping. The number of these groups is indicated by the symbol Δ . This behaviour can be empirically obtained by numerical simulations, with a standard pseudorandom variate procedure algorithm [20] through the generation of a synthetic sequence consisting of N real values dependent on the parameter λ of the distribution $P(X, \lambda)$. In order to evaluate the TPL, the sequence of real values is partitioned into Δ nonoverlapping subgroups, each of length $d\Delta$, which is the ratio between N and Δ . Next, for each of these subgroups, we compute aggregate measures, namely the mean μ and the variance σ^2 . It is observed that for synthetic values of $10^4 \leq N \leq 10^6$ and $10^3 \leq \Delta \leq 10^5$, the presence of periodic components within the TPL depends solely on the value of the mean, μ , in a domain in which σ^2 belongs to the interval (0, 1). With $N = 10^6$ and for the distribution (1), the values of the mean, μ , which manifests a TPL with periodic components fall within a range (0.5, 10). For values of $\mu \leq 1$ it assumes periodic characteristics that belong to Bernoulli distributions. According to Hughes and Madden [16], TPL takes on a singular behaviour with this distribution that can be characterised as a subset of the Poisson distribution and thus a limiting case of the binomial (with probability p), where the expected value is $\mathbb{E}(X) = p$ and the variance is $Var(X) = p(1 - p)$, while a and b are equal to 1. In Fig. 1 the blue line represents the TPL interpolation law, namely $\log(\sigma^2) = \log(a) + b \log(\mu)$, which, in this specific case for $N = 10^6$, with $\Delta = 10^5$, and $\lambda = 2$, takes on the numerical value of $a = 0.997 \pm 0.003$ and $b = 1.00 \pm 0.001$, while the modulated curves in cyan, green and red represent periodic interpolation functions whose meaning will be explained in the next section. Fig. 2A shows the periodic behaviour of the TPL generated through the $P(X, \lambda)$ distribution for $N = 10^6$, $\Delta = 10^5$, $\lambda = 1$, $a = 1$ and $b = 1$. Fig. 2B shows instead a TPL with Bernoulli distribution obtained from a synthetic data set for $N = 10^6$, $\Delta = 10^5$ and with probability parameter $p = 0.7$, $a = 1$ and $b = 1$. It can be observed directly from the comparison of the two figures how the TPL with Bernoulli distribution is a limiting case of $P(X, \lambda)$ when the mean, μ , takes values between 0.1 and 1, with $\sigma^2 \leq 1$. In both figures, the parameters a and b are equal to unity. While Fig. 2C shows the trend of TPL generated through the $P(X, \lambda)$ distribution for $N = 10^6$, $\Delta = 10^5$, $\lambda = 20$, $a = 1$ and $b = 0.997$. This last significant step shows how as the mean values increase, μ , in each of the Δ partitions there is a loss of periodic components, with a transition towards greater complexity dictated by TPL as a whole. Many of the latter configurations can be found in Taylor [2].

2.2. The case of TPL with binomial and other distributions

The emergence of this singular behaviour is also typical of other distributions such as the binomial, of which the Poissonian is a particular case when the number of trials n increases indefinitely whilst the product $\mu = np$, which is the expected value of the number of successes from the trials, remains constant. By operating on the modulation parameters, one can obtain a number, however finite, of solutions that succeed in mapping the graph, the superposition of which provides the periodic plane of TPL when $b = 1$. Specifically, consider the binomial probability mass function:

$$B(X; n, p) = \frac{n!}{(n - X)!X!} p^X (1 - p)^{n - X} \quad (2)$$

it could be easily demonstrated that relation (1) is a limit case of relation (2) when $n \rightarrow \infty$ and $p \rightarrow 0$. Through $B(X; n, p)$, it is possible to obtain the same periodic scenarios as $P(X, \lambda)$. Figs. 3A, 3B and 3C show some cases of TPL with $B(X; n, p)$. The generation of the TPLs was implemented as in the previous case, with a random sequence of $N = 10^6$ real values, with a maximum of 10^5 partitions (Δ), and with $n = 10$, $p = 0.1$, $p = 0.3$ and $p = 0.5$. Even in this second case, which generalises the first, periodicities are evident in

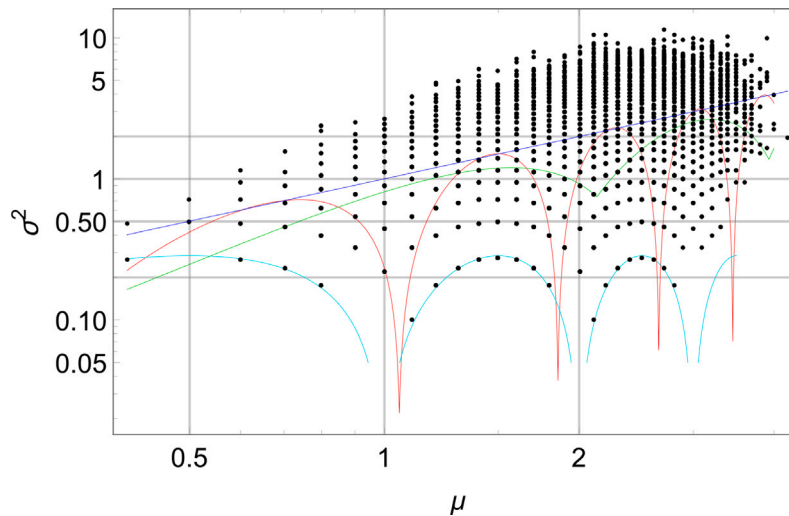


Fig. 1. σ^2 vs μ , in logarithm scale, of $N = 10^6$ real numbers of X (black points) distributed according Eq. (1) with $\lambda = 2$ and $\Delta = 10^5$. Modulated curve in cyan is obtained from Eq. (3) with $\delta = 0.3$ and $\zeta = (\pi/11\delta)$. Modulated curve in green is obtained from Eq. (5) with $\alpha = 0.35$, $\beta = 0.5$, $K = 3.5\pi/5.4$, $d = -10$ and $b = 1$. Modulated curve in red is obtained from Eq. (6) with $\xi = 0.02$, $\gamma = 1$, $\theta = 5\pi/4$, $\eta = -1$, $a = 1$ and $b = 1$.

Table 1

Parameters of distributions with periodic components and a and b values of TPL. For the Zipf-discrete-Pareto distribution ρ is a positive real parameter. All simulations were generated through a standard pseudorandom variate procedure algorithm [20] for 10^6 random values with a maximum 10^5 aggregate groups.

Distributions	n	p	ρ	a	b
Zipf-discrete-Pareto			2.4	1.493	2.624
Pascal	3	0.6		0.016	3.293
Geometric		0.3		1	1
Negative-binomial	2	0.5		1.322	1.534

the logarithmic plane (σ^2 vs. μ), where a and b are equal to 1 in the case of Fig. 3A, while in Figs. 3B and 3C the parameters a and b are equal to 1.153, 2.462, and 0.547, 0.01, respectively. We note that in the case of the binomial distribution the TPL assumes for values of the probability, $p \geq 0.5$, a behaviour of $b \sim 0$. Therefore, as the probability, p , increases, for $n = \text{const.}$, there is a reduction in the aggregation index b tending towards Gaussian behaviour, and this is in agreement with the observations by Tweedie [3]. Moreover, it is observed that manifestations of periodic components can be observed numerically in TPL sub-domains ($\sigma^2 \leq 1$) with the following distributions: Zipf-discrete-Pareto ($b > 2$ and $a > 1$), Pascal ($b > 3$ and $a > 0$), Geometric ($b = 1$ and $a = 1$) and Negative-binomial ($b > 1$ and $a > 1$). Fig. 4 show the numerical results for the above mentioned distributions for simulations with $N = 10^6$ random real elements and a maximum number of partitions, Δ , equal to 10^5 . The setting parameters for the distributions listed above are reported in Table 1 in which the estimated values of a and b are also summarised. From this analysis, and in all the studied cases, it is possible to observe graphically how for σ^2 tending to 1 we obtain the maximum harmonic component. While, the most important aspect that emerges from all these simulations is that the peak value of the variance σ^2 related to the first basic harmonic component, and for each distribution analysed, takes on the constant value of 0.3. The latter aspect, somewhat surprising, seems to indicate an emerging universality in other physical contexts including braided channel network systems (BCNs), as recently shown in experimental investigations by De Bartolo et al. [14] and Rizzello et al. [17]. In the light of these new analyses conducted here on binomial type distributions, the emerging behaviour of 0.3 appears to be a peak property of the first periodic component, not only for $P(X, \lambda)$ and $B(X; n, p)$, but also of all distributions attributable to them for 10^6 data and for small TPL aggregation measures in which σ^2 turns out to be in the neighbourhood of 1.

3. Periodic variances and analysis of components

The observations highlighted in the previous section show that in the vicinity of TPLs distributed according to the density functions, $P(X, \lambda)$ and $B(X; n, p)$, for a variance $\sigma^2 \sim 1$, the periodic components emerge in the lower part of the logarithmic plane (σ^2 versus μ). Moreover, as already anticipated, also other TPLs associated to different distributions with $b > 1$ exhibit periodic components: they can still be traced back to the binomial with variance σ^2 close to one. Recently, these cases (denoted

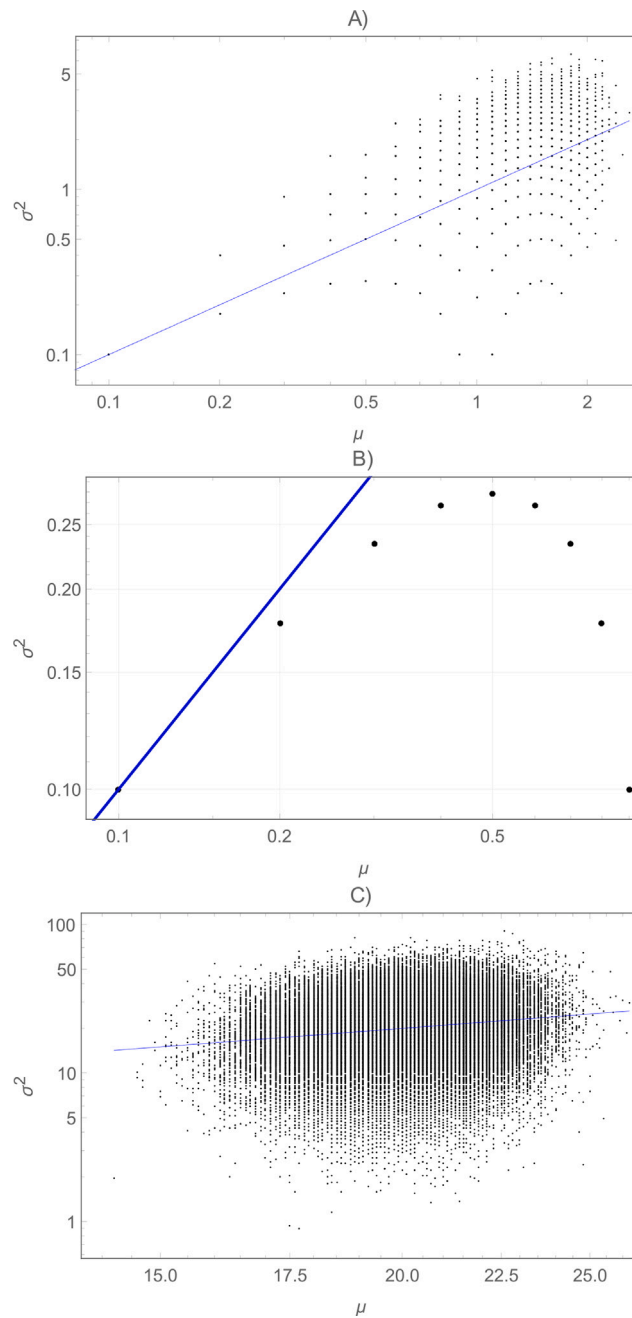


Fig. 2. Fig. 2A shows a TPL generated through the $P(X, \lambda)$ distribution for blue $N = 10^6$, $\Delta = 10^5$ and $\lambda = 1$. Fig. 2B shows a TPL with Bernoulli distribution obtained from a synthetic data set for $N = 10^6$, $\Delta = 10^5$ and with probability parameter $p = 0.7$. Fig. 2C shows a TPL generated through the $P(X, \lambda)$ distribution for $N = 10^6$, $\Delta = 10^5$ and $\lambda = 20$.

as ‘singularities’ in this work) have reemerged in some physical contexts, as reported in [14,17]; this induces the presence of a periodicity into one of the parameters of the TPL or, rather, in a behaviour transition that starts essentially from a periodic-type behaviour of the variance. In particular, this can be observed in the neighbourhood of 1 towards greater complexity dictated by a TPL, in the upper part of the domain with $\sigma^2 > 1$ and with $b \geq 1$. This behaviour can be interpreted through three different scenarios. That, starting from a basis with periodic μ -dependent components that we will call the first deterministic part, can transit to two other possible deterministic scenarios dependent on the periodic conditions of $a(\mu)$ and a multiplicative process within the TPL.

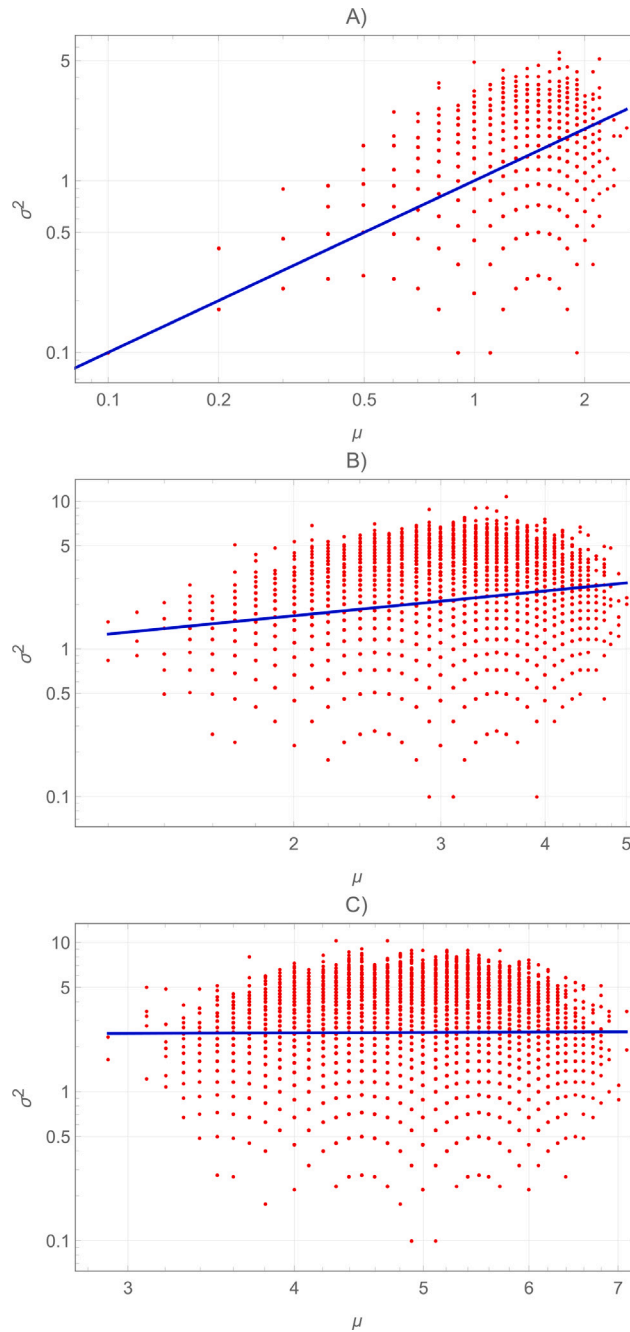


Fig. 3. σ^2 vs μ , in logarithmic scale, of 10^6 real numbers of X (red points) distributed according to relation (2), with $\Delta = 10^5$. Fig. 3A was generated with $n = 10$ and $p = 0.1$. Fig. 3B was generated with $n = 10$ and $p = 0.3$, while Fig. 3C was generated with $n = 10$ and $p = 0.5$.

3.1. Interpretive scenarios of periodic patterns

The first scenario, that has already emerged in the work of De Bartolo et al. [14] and Rizzello et al. [17], is based on a variance relation, σ^2 , of the type:

$$\sigma^2 = \zeta \delta |\sin(\pi\mu)| \tag{3}$$

where, ζ and δ are real parameters of modulation. Eq. (3) provides a good approximation of the basic periodic components of TPL obtained from relation (1). In Fig. 1 the function in cyan was obtained for $\delta = 0.3$ and $\zeta = \pi/(11\delta)$.

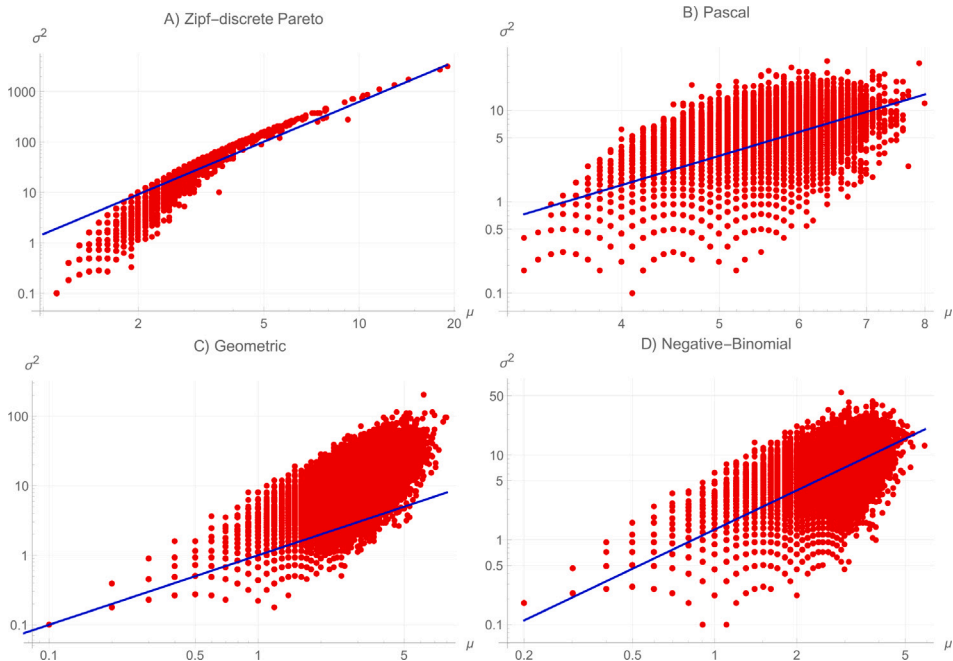


Fig. 4. σ^2 vs μ , in logarithm scale, of 10^6 real values of X (red points) distributed according Zipf-discrete-Pareto (A), Pascal (B), Geometric (C) and Negative-binomial (D) distributions.

The second scenario is to consider in TPL the coefficient a as a periodic function of μ . Thus, we can define a as a sinusoidal function of μ :

$$a(\mu) = \alpha + \beta |\sin(K\mu + d)|, \quad (4)$$

then, the TPL becomes

$$\sigma^2 = (\alpha + \beta |\sin(K\mu + d)|)\mu^b, \quad (5)$$

where α is a real parameter, β controls the amplitude, K the frequency and d the phase shift of the periodic component, respectively. In Eq. (5) when we set $b = 1$ for Binomial and Poisson distributions this means that we consider a linear relationship modulated by a periodic coefficient. For instance, in the case shown in Fig. 1, the curve in green shows Eq. (5) plotted for $\alpha = 0.35$, $\beta = 0.5$, $K = 3.5\pi/5.4$, $d = -10$, and $b = 1$. This plot will show how the variance, σ^2 , varies with the mean, μ , in a periodic manner. The sinusoidal component in $a(\mu)$ causes the variance to oscillate as the mean increases. This shows how periodicity can be introduced into the relationship between variance and mean, reflecting TPL scenarios where the underlying factors influencing the system are themselves periodic. By operating on the modulation parameters, one can obtain a number, however finite, of solutions that succeed in mapping the graph, the superposition of which provides the periodic plane of TPL when $b = 1$.

The third scenario can be provided by a periodic variability of a multiplicative process within TPL. Therefore Eq. (5) becomes:

$$\sigma^2 = (\xi + \gamma |\sin(\theta\mu + \eta)|)a\mu^b \quad (6)$$

with ξ , γ , θ and η are modular real parameters analogous to (5). In Fig. 1 the red modular curve was obtained from Eq. (6) with $\xi = 0.02$, $\gamma = 1$, $\theta = 5\pi/4$, $\eta = -1$, $a = 1$ and $b = 1$. It is important to emphasise that, in all the cases analysed, the slope line b of the TPL marks a boundary separating the part of the graph with 'periodic components', lower part of the figure, from that of the power law proper, higher part. It is also observed that the modulation curves described through the relations (3), (5), and (6) exhibit an overlap confined below the slope line of the TPL that represents its tangent. In the next section, a theoretical explanation will be provided to justify the formation of periodic patterns within certain TPLs.

4. Differences between variance and mean in small aggregation processes

The TPL processes emphasised in the previous sections are characterised by fluctuating physical phenomena whose number of subgroups, Δ , are small compared to the entire sampling space of the same processes in space or time. The size of these subgroups are denoted by $d\Delta$. Scaling of subgroup sizes to determine periodic patterns represents the core of this behaviour, which can be summarised as follows. For fluctuating sequences, X , positively defined, for which TPL is applicable, the partitions over small subgroups, Δ , will be characterised by a variability of the type $X + k$, where k is a real constant to be evaluated. This implies that as

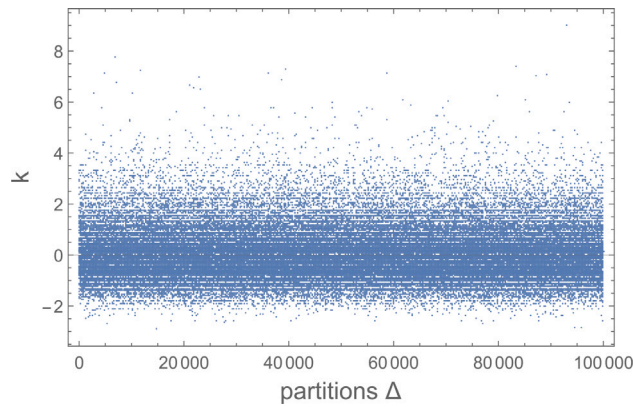


Fig. 5. Behaviour of the relation (9) obtained from a TPL with Poissonian distribution of $N = 10^6$ random data, with $\lambda = 2$, $\Delta = 10^5$, and $d\Delta = 10$.

the size of the subgroups increases, with however small size increments $d\Delta$, we will have for μ , or expected value, \mathbb{E} , the following relation:

$$\mu(X + k) = \mathbb{E}(X + k) = \mathbb{E}(X) + k, \quad (7)$$

and this means that with each further Δ , we add a constant value on μ . Similarly, we can write the variance, σ^2 , or $\text{Var}(X)$ as:

$$\sigma^2(X + k) = \text{Var}(X + k) = \text{Var}(X). \quad (8)$$

For measure supports with Poissonian distributions ($\sigma^2 = \mu$), and for small values of the size $d\Delta$ of a subgroup, the value that induces the periodic component is due to the fact that the constant value is equal to:

$$k = \text{Var}(X) - \mathbb{E}(X). \quad (9)$$

Thus, the TPL takes on a form defined in the plane (σ^2 vs. μ) and determined by a definite range of values of k varying from 0 to $\pm m$, where the latter still takes on a finite real value dependent on the sampling under consideration. Fig. 5 shows this behaviour for a TPL generated with a Poissonian distribution obtained from $N = 10^6$ random data, with $\lambda = 2$, $\Delta = 10^5$, and $d\Delta = 10$. The investigation conducted here reveals a nonlinear functional relation $k = f(d\Delta)$ naturally describable by a power law of the type:

$$k = \omega d\Delta^{-\phi}, \quad (10)$$

in which ω is a constant factor and ϕ a scaling exponent. The scaling associated with the relation (10) can be of two types, the first for positive m and the second for negative m . This duality is a fundamental achievement as it allows the recognition of the limit of separation between the behaviour of TPL with periodic patterns from that one without. Specifically, a numerical simulation was carried out by considering a TPL distributed through the Poissonian distribution, $P(X, \lambda)$, for $\lambda = 2$, by varying the number of partitions, Δ , and thus the size of the subgroups, $d\Delta$. For the data $N = 10^6$, the following partitions $\Delta \in [5 \cdot 10^5, 2.5 \cdot 10^5, 2 \cdot 10^5, 10^5, 5 \cdot 10^4, 4 \cdot 10^4, 2 \cdot 10^4, 10^4, 5 \cdot 10^3, 4 \cdot 10^3, 2 \cdot 10^3]$ were analysed with the corresponding $d\Delta \in [2, 4, 5, 10, 20, 25, 50, 100, 200, 250, 500]$. The numerical results show a bimodal behaviour of the scaling process, characterised in both cases (see Fig. 6 A, B, C) by a separation point at the abscissa $d\Delta = 25$. The latter represents the cut-off limit value with respect to which the aforementioned curves not only assume different slopes but also define the ranges in which the behaviour of the TPL does not assume periodic patterns. Therefore, for values of $d\Delta$ included in the interval $[2 - 25]$ the TPL manifests periodic patterns, while for $d\Delta > 25$ the TPL loses its periodic components. Fig. 6A shows the positive scaling of k vs. $d\Delta$, and Fig. 6B the negative one. In both Figures, one can observe the change of slope in the aforementioned separation point, that is clearly evident in the logarithmic scale of the relationship (10) depicted in Fig. 6C. Similar considerations can be obtained from the scaling expressed by Fig. 6B and thus from the negative values of k . In the case of positive k values the parameters estimated by means of the power law (10) were $\omega = 88.10$ and $\phi = 0.954$ for the scaling representing the periodic patterns (first scaling range) and $\omega = 21.71$ and $\phi = 0.605$ for the second scaling representing the absence of the first ones (second scaling range). While in the case of negative k values the parameters are $\omega = -12.10$ and $\phi = 0.638$ for the scaling representing the periodic patterns (first scaling range) and $\omega = -12.85$ and $\phi = 0.572$ for the second scaling range indicating the lack of periodic patterns. In both scaling ranges analysed the determination coefficient R^2 was very close to unity. Figs. 7A and 7B show the respective TPLs in the transition part from behaviour with periodic patterns to behaviour without periodic patterns.

Summarising, the numerical investigation has revealed that the behaviour of TPL distributed according to Poissonian probability density functions, $P(X, \lambda)$, exhibits periodic patterns when the sequence of the random variable, X , is clustered in particular subgroups characterised by small size $d\Delta$ when related to the entire sampling length. The range of separation is provided by the bimodal scaling represented by the power law (10) at a particular separation point separating the parts.

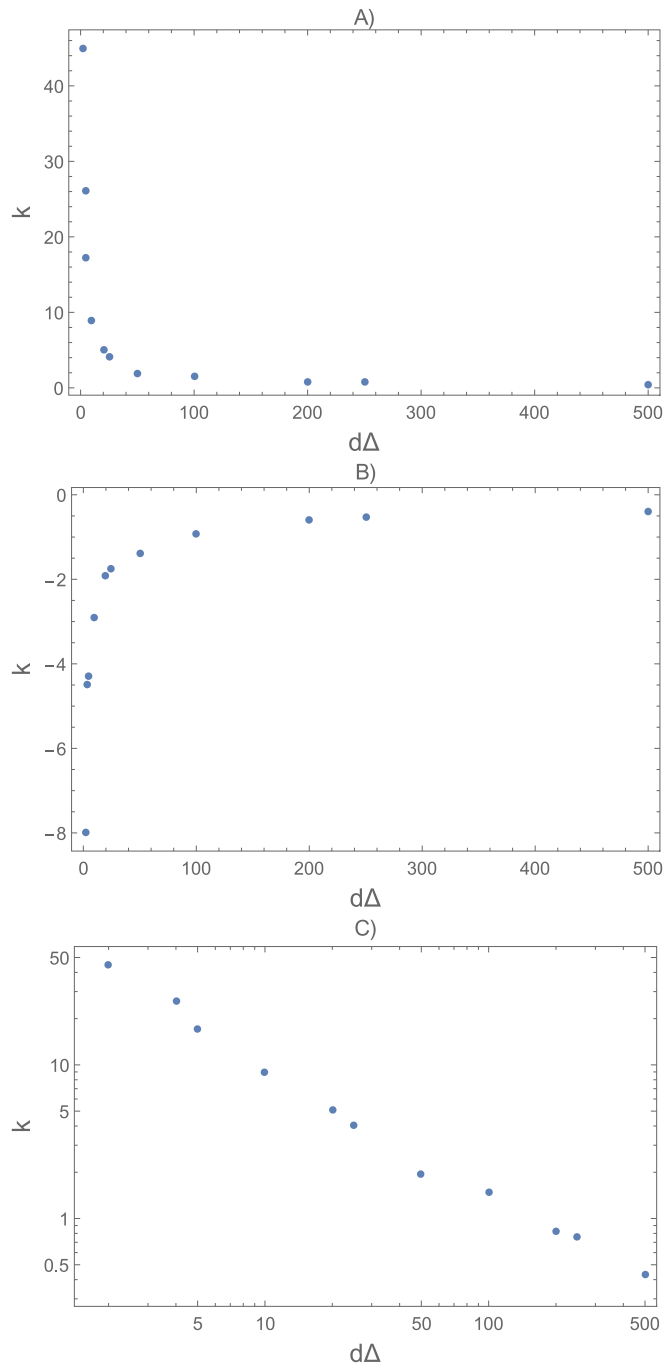


Fig. 6. Behaviour of the relation (10) obtained from a TPL with Poissonian distribution of $N = 10^6$ data and $\lambda = 2$. Fig. 6A shows the trend of positive k versus $d\Delta$, while Fig. 6B shows the trend of negative ones. Fig. 6C represents Fig. 6A in the logarithmic plane.

5. Discussion of other specific cases

5.1. TPL with Bernoulli distribution

Interesting aspects can be observed regarding TPL with Bernoulli distribution. In this case, the TPL depends on the probability parameter p . By means of a simulation represented by a synthetic construction of $N = 10^6$ random data with $\Delta = 10^5$ subgroups, three values of the probability parameter p were taken into account, namely the values 0.1, 0.5, and 0.95. The simulation made it

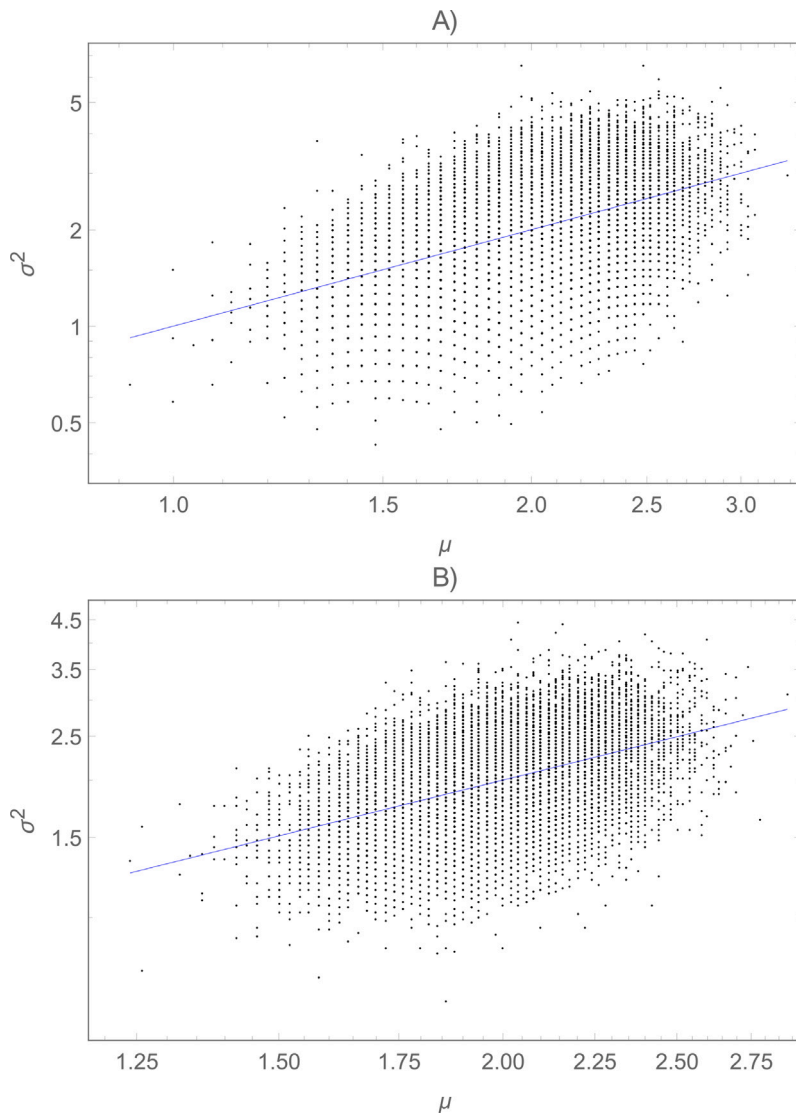


Fig. 7. TPL obtained from Poissonian distributions for $\lambda = 2$ and $N = 10^6$. Fig. 7A shows the case for $\Delta = 4 \cdot 10^4$ and $d\Delta = 25$, with periodic patterns. Fig. 7B shows the case for $\Delta = 2 \cdot 10^4$ and $d\Delta = 50$ without periodic patterns.

possible to assess the range of variability of the difference between variance and mean represented by the parameter k , relation (9). The results show a definite trend in the k value as the probability p varies. In all three cases k takes on negative values in the range $(-1, 0)$. Figs. 8A, 8C, 8E show these trends. It is significant to acknowledge that there is a substantial shift of k values calculated with a higher density in the range evaluated for $p = 0.5$. In any case, the most important element that emerges from this analysis is that TPL with Bernoulli distributions can be described, as a first cycle, by the harmonic variance relations represented by Eqs. (3), (5) and (6). Fig. 9 shows how relation (3) provides a good interpolation ($R^2 \sim 1$) of the TPL obtained by Bernoulli distribution for $N = 10^6$ random data, $\Delta = 10^5$ subgroups and probability $p = 0.5$. The setting parameters for relation (3) are $\delta = 0.3$ and $\zeta = \pi/(11\delta)$. This singular behaviour fits into a more general context of similarity between TPL with Poissonian distribution and with Bernoulli distribution, the latter being a special case of the former in the domain ($\sigma^2 \in (0.10, 1)$ vs, $\mu \in (0.1, 1)$).

5.2. Braided channel networks: Allaro River study case

In the studies by De Bartolo et al. [14] and Rizzello et al. [17] the first cases of TPL characterised by harmonic patterns were found. The investigation of numerous braided channel systems has tended to show multiscaling behaviour of some very important geomorphological descriptors suitable for the dynamic description of these systems. The hydraulic random variables X taken into account were three, namely the number of wet channels, N_{wc} , the average wetted width, w_{wc} , and the entropic braided index, EBI.

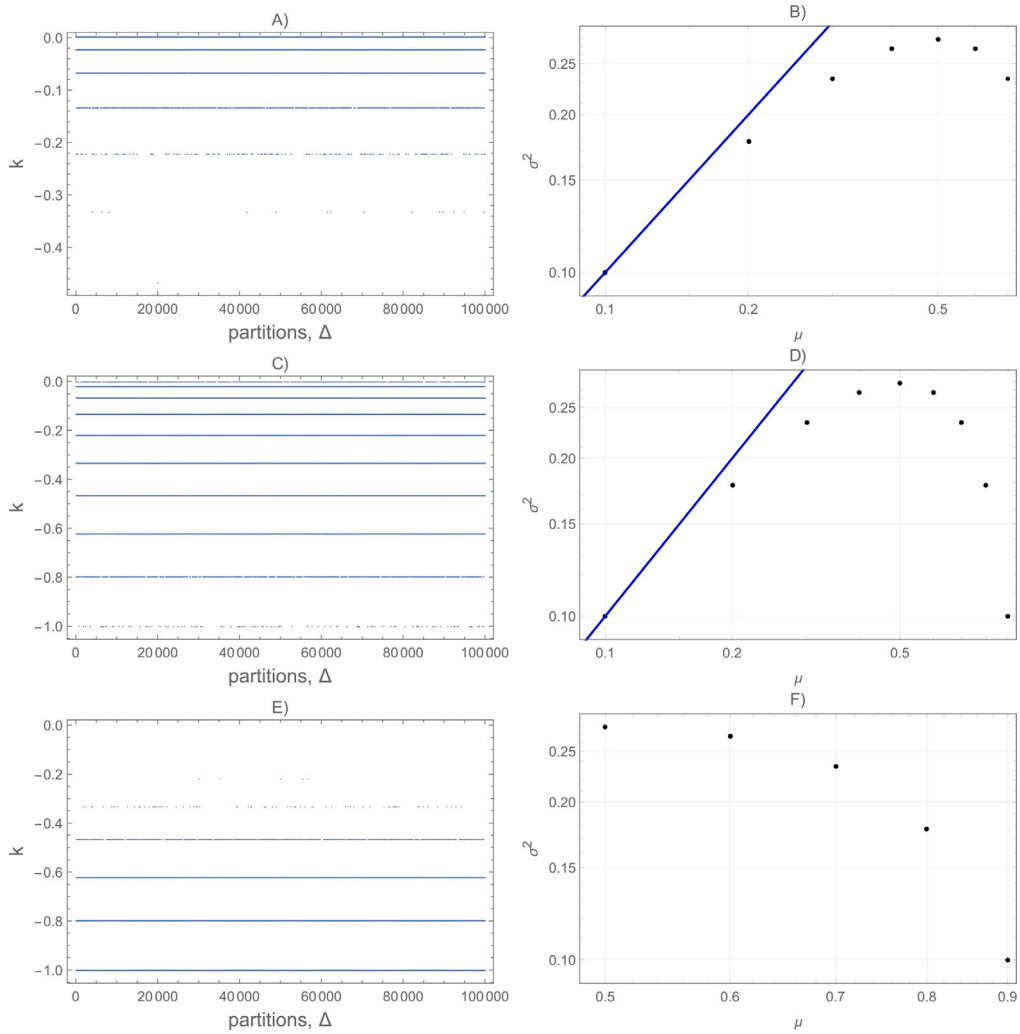


Fig. 8. Behaviour of the relation (9) obtained from a TPL with Bernoulli distribution of $N = 10^6$ random data. Figs. 8A, 8C and 8E show the trend of negative k versus Δ . Figs. 8B, 8D and 8F show the three TPLs obtained through the p values of 0.1, 0.5 and 0.95 respectively.

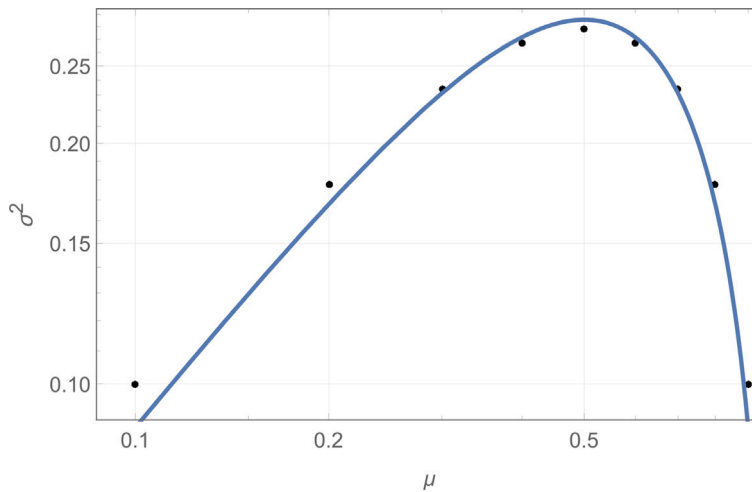


Fig. 9. TPL with Bernoulli distribution of $N = 10^6$ random data, obtained through the p values of 0.5. The interpolating curve in blue was obtained using relation (3) with the following parameters: $\delta = 0.3$ and $\zeta = \pi/(11\delta)$.

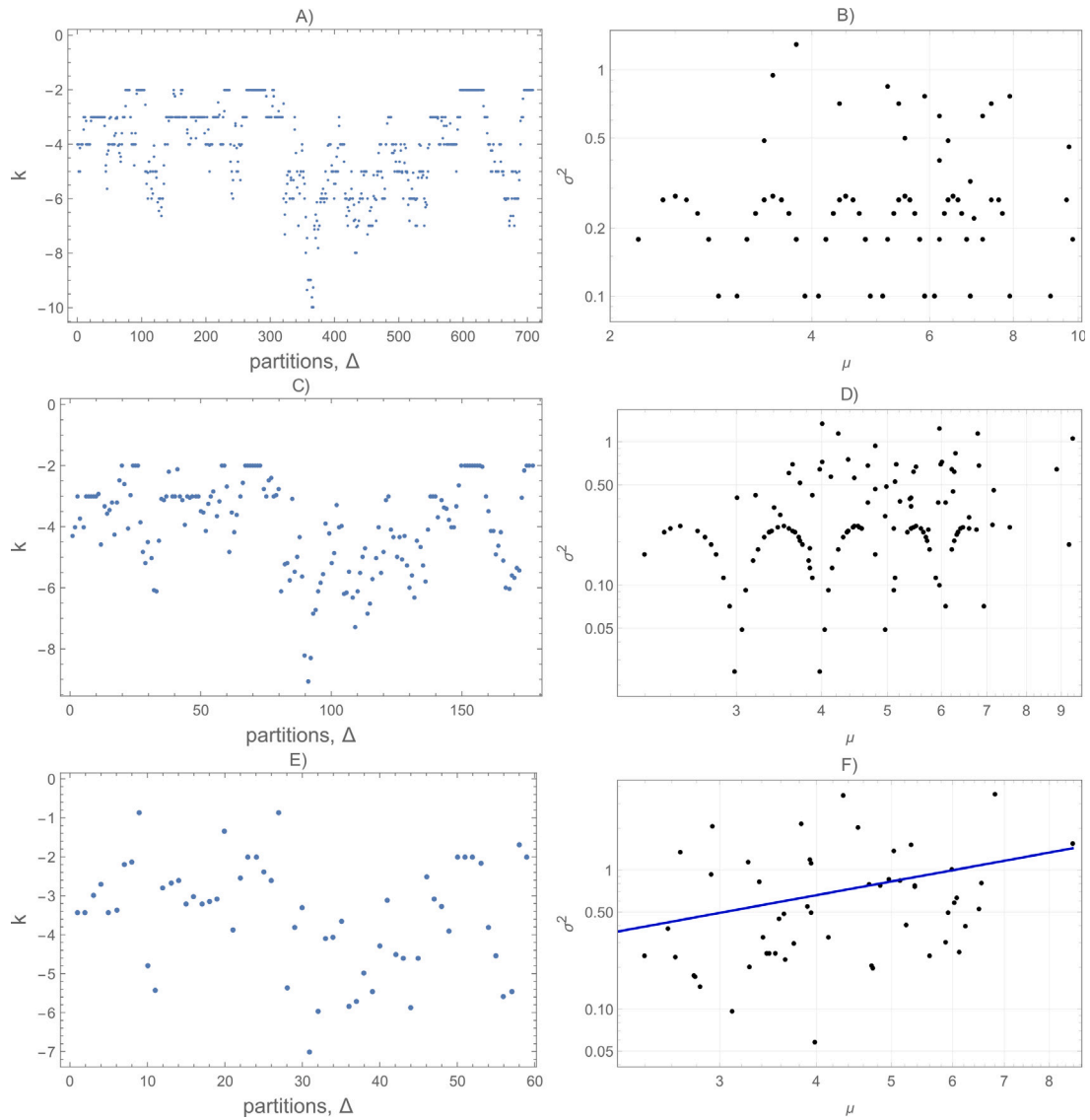


Fig. 10. Experimental analysis conducted on the Fiumara Allaro.

All three variables assume a non-zero mean random behaviour in space. For the definitions of these geomorphological descriptors, please refer directly to the aforementioned works. Specifically, it has been observed that for aggregations, however small compared to the scale of extraction of the whole river channel network, the behaviour of TPL takes on periodic components, as in the cases mentioned above. This means that for a certain number of spatial subgroups, Δ , gradually increasing but still small compared to the scale of the entire sequence of the network, we add a constant integer number of channels. In this subsection we take up the case of the Fiumara Allaro, which represents a significant case of TPL transition characterised by behaviour with periodic patterns towards Poissonian distributions. In De Bartolo et al. [14] the scaling relative to this behaviour was shown. Here we take up some significant passages showing the behaviour of the relation (9) in the context of the number of wet channels, N_{wc} , analysed within some significant Δ partitions. The analysis resumed here shows the behaviour of TPL for three distinct cases over a total number of $N = 7081$ elements equispaced at a distance of 1 metre between measurement cross-sections, totalling approximately 7 km. The first case concerns $\Delta = 708$ subgroups with size of $d\Delta = 10$ m, the second case is characterised by $\Delta = 177$ subgroups with size $d\Delta = 40$ m and finally the third with $\Delta = 59$ subgroups with size $d\Delta = 120$ m. Figs. 10 A, 10 C and 10 E show, for the three cases analysed, the behaviour of the difference between variance and mean for each partition, i.e. the variable k . It is significant to note that this variable behaves differently from the cases analysed previously and can be framed as intermittent in the range of negative values only. Essentially, this implies that the mean increases more than the variance with a certain cyclicity for tendentially small $d\Delta$ values (see Fig. 10 A). Figs. 10 B, 10 D and 10 F show the corresponding TPL behaviours for the assigned partitions. Therefore,

it can be stated that in the case of braided channel networks the transition to TPL with Poissonian distribution, such as the case hypothesised in Fig. 9 F, occurs with a periodic decrease in the mean, μ , and thus the basic periodic component can be described through the relation (3) for sizes of the subgroups between approximately 5 m and 40 m. In this context, it is significant to show that the peak value is 0.3.

The results obtained here in accordance with the works [14,17,21] confirm what has already been pointed out in previous cases, namely that the presence of periodic patterns for distributions that tend towards the Poissonian and hence the binomial depends essentially on the size of the aggregation subgroups measures, when these are small enough with respect to the entire sampling taken into consideration.

6. Conclusion

In conclusion, in this work it was shown how some Taylor Power Laws (TPLs) can take on in the bilogarithmic plane (σ^2 vs. μ) behaviour with 'periodic patterns' of variance. These TPLs belong to the category of binomial type distributions and some traceable to it as a limiting case, including the Poissonian distribution of which it is known that the aggregation index of the TPL b is equal to 1. The numerical investigation was also extended to other TPLs with distributions traceable to the binomial, including Bernoulli and Pascal, on the basis of synthetic simulations consisting of 10^6 elements, with 10^5 subgroups. Periodic patterns were also observed in these cases. Based on the experiences of Taylor and Woiwod [15], Hughes and Madden [16], De Bartolo et al. [14] and Rizzello et al. [17], three interpretative scenarios of this behaviour were provided. In particular, both for the experimental results observed in De Bartolo et al. [14] and Rizzello et al. [17] and for the numerical results obtained by TPL with Poissonian distributions, the first proposed scenario provided good interpolations ($R^2 \sim 1$) of the basic periodic component. In general, it has been observed that this behaviour is a process resulting from successive partitions of the TPL, characterised by small size $d\Delta$ relative to the entire length of the sequence of measures. Therefore, the phenomenon was further investigated by studying the variance, σ^2 , and mean, μ , measured in each partition minus a real parameter, k , obtained as the difference between the two. This approach made it possible to determine the direct scaling between k and the size $d\Delta$ by means of a particular power law. This law showed a bimodal behaviour of the measured values through which it was possible to trace the size of the subgroups in which TPL manifests a periodic and non-periodic pattern. Bimodality, characterised by a particular separation point, was shown for positive and negative k values. In both cases the results converged to define the existence of a certain range of sizes in which the behaviour of TPL takes on periodic patterns. The investigation also made it possible to characterise TPLs with Bernoulli distributions as a particular periodic case of TPLs with Poissonian distributions in the domain ($\sigma^2 \in (0.10, 1)$ vs. $\mu \in (0.1, 1)$). It was also shown how in the context of all the distributions analysed, the TPLs show a constant behaviour of the peaks of the first basic component, and that this value is very close to 0.3. To confirm this behaviour, a further experimental case was shown regarding the analysis conducted by De Bartolo et al. [14] for the braided Allaro River.

CRedit authorship contribution statement

Samuele De Bartolo: Writing – review & editing, Writing – original draft, Visualization, Validation, Supervision, Software, Methodology, Investigation, Formal analysis, Data curation, Conceptualization.

Declaration of competing interest

The authors declare that they have no known competing financial interests or personal relationships that could have appeared to influence the work reported in this paper.

Data availability

Data will be made available on request.

Acknowledgements

I would like to thank the two anonymous reviewers and the main editor Dr. Michael Small for their comments and valuable suggestions during the revision phase of this work.

References

- [1] L.R. Taylor, Aggregation, variance and the mean, *Nature* 189 (1961) 732–735.
- [2] R.A.J. Taylor, *Taylor's Power Law, Order and Pattern in Nature*, Academic Press, 2019.
- [3] M.C.K. Tweedie, An index which distinguishes between some important exponential families, *Statist.: Appl. New Directions* 32 (1984) 3397–3408.
- [4] B. Jørgensen, Exponential dispersion models, *J. R. Statist. Soc. Ser. B* 49 (1987) 116–127.
- [5] W.S. Kendal, A probabilistic model for the variance to mean power law in ecology, *Ecol. Model.* 80 (1995) 293–297.
- [6] W.S. Kendal, A stochastic model for the self-similar heterogeneity of regional organ blood flow, *Proc. Natl. Acad. Sci. USA* 98 (3) (2001) 837–841.
- [7] W.S. Kendal, Spatial aggregation of the Colorado potato beetle described by an exponential dispersion model, *Ecol. Model.* 151 (2002) 261–269.
- [8] E. Zoltán, I. Bartos, J. Kertész, Fluctuation scaling in complex systems: Taylor's law and beyond, *Adv. Phys.* 57 (1) (2008).
- [9] A. Fronczak, P. Fronczak, Origins of Taylor's power law for fluctuation scaling in complex systems, *Phys. Rev. E* 81 (6) (2010).

- [10] W.S. Kendal, B. Jørgensen, Taylor's power law and fluctuation scaling explained by a central-limit-like convergence, *Phys. Rev. E* 83 (2011).
- [11] W.S. Kendal, B. Jørgensen, Tweedie convergence: A mathematical basis for Taylor's power law, $1/f$ noise, and multifractality, *Phys. Rev. E* 84 (2011).
- [12] A. Giometto, M. Formentin, A. Rinaldo, J.E. Cohen, A. Maritan, Sample and population exponents of generalized Taylor's law, *Proc. Natl. Acad. Sci. USA* 112 (25) (2015).
- [13] B. Jørgensen, *The Theory of Dispersion Models*, Chapman & Hall, 1997.
- [14] S. De Bartolo, S. Rizzello, E. Ferrari, F. Frega, G. Napoli, R. Vitolo, M. Scaraggi, C. Fallico, Severino, scaling behaviour of braided active channels: a Taylor's power law approach, *Eur. Phys. J. Plus* 137 (2022) 622.
- [15] L.R. Taylor, I.P. Woiwod, Comparative sinoptic dynamics. I. Relationships between inter-and intra-specific spatial and temporal variance/mean population parameters, *J. Animal Ecol.* 51 (1982) 879–906.
- [16] G. Hughes, L.V. Madden, Aggregation and incidence of disease, *Plant Pathol.* 41 (1992) 657–660.
- [17] S. Rizzello, M. Scaraggi, A.D. Nelson, P. Primavera, G. Napoli, G. Stecca, R. Vitolo, S. De Bartolo, Multiscaling behavior of braided channel networks: An alternative formulation of Taylor's law variate transformations, *Phys. Rev. E* 109 (2024) 034306.
- [18] I. Eliazar, Harmonic statistics, *Ann. Phys.* 380 (2017) 168–187.
- [19] I. Eliazar, *Power Laws, a Statistical Trek*, Springer, 2020, pp. 199–203, Chap. 18.
- [20] Wolfram Research, *RandomVariate*, *Wolfram Language Function*, 2010, <https://reference.wolfram.com/language/ref/RandomVariate.html>.
- [21] S. De Bartolo, C. Fallico, E. Ferrari, Simple scaling analysis of active channel patterns in Fiumara environment, *Geomorphology* 232 (2015) 94–102.